Procedia Computer Science

Volume 29, 2014, Pages 991–1001

ICCS 2014. 14th International Conference on Computational Science

Micropolar Fluids using B-spline Divergence Conforming Spaces

Adel Sarmiento[1,3], Daniel Garcia[2,3], Lisandro Dalcin[3], Nathan Collier[3], and Victor Calo[1,3,4]

[1] Applied Mathematics & Computational Science, King Abdullah University of Science and Technology (KAUST), Thuwal, Saudi Arabia
adel.sarmientorodriguez@kaust.edu.sa

[2] Mechanical Engineering, King Abdullah University of Science and Technology (KAUST), Thuwal, Saudi Arabia
daniel.garcalozano@kaust.edu.sa

[3] Center for Numerical Porous Media (NumPor), King Abdullah University of Science and Technology (KAUST), Thuwal, Saudi Arabia
dalcinl@gmail.com, nathaniel.collier@gmail.com

[4] Earth Science & Engineering, King Abdullah University of Science and Technology (KAUST), Thuwal, Saudi Arabia
victor.calo@kaust.edu.sa

Abstract

We discretized the two-dimensional linear momentum, microrotation, energy and mass conservation equations from micropolar fluids theory, with the finite element method, creating divergence conforming spaces based on B-spline basis functions to obtain pointwise divergence free solutions [8]. Weak boundary conditions were imposed using Nitsche's method for tangential conditions, while normal conditions were imposed strongly.

Once the exact mass conservation was provided by the divergence free formulation, we focused on evaluating the differences between micropolar fluids and conventional fluids, to show the advantages of using the micropolar fluid model to capture the features of complex fluids. A square and an arc heat driven cavities were solved as test cases. A variation of the parameters of the model, along with the variation of Rayleigh number were performed for a better understanding of the system.

The divergence free formulation was used to guarantee an accurate solution of the flow. This formulation was implemented using the framework PetIGA as a basis, using its parallel stuctures to achieve high scalability. The results of the square heat driven cavity test case are in good agreement with those reported earlier.

Key words: Divergence-conforming B-splines, isogeometric finite element method, micropolar fluids, incompressible flows, divergence free.

Keywords:

Selection and peer-review under responsibility of the Scientific Programme Committee of ICCS 2014

doi:10.1016/j.procs.2014.05.089

Contents

1 Introduction

Micropolar fluids are a subclass of simple microfluids presented by Eringen [1], that have gained attention from researchers because they can succesfully model the behavior of non-Newtonian fluids like ferro liquids, liquid polymers, and any fluid with suspended particles in it. One of many applications is to model nanofluids, where inserting nanoparticles can change physical properties in a desired way depending on the volume fraction of the nanoparticles. Like is the case of fluid heat transfer systems where nanoparticles are added to increase the effective heat conductivity for numerous applications. Nanofluids are better modeled using the micropolar fluids theory. This takes into account the conservation of angular momentum of the nanoparticles that are not described by the regular Navier-Stokes equations.

Micropolar fluids consist of randomly oriented particles submerged in a viscous fluid where the deformation of the particles is neglected. Here we present the results for an isotropic, incompressible micropolar fluid to represent the steady state of natural convection in the heat driven cavity, using Boussinesq approximation for buoyancy effects. We modelled the system using the finite element method with B-splines basis functions, where to satisfy the Ladyzhenskaya-Babuska-Brezzi (LBB) condition we used a divergence conforming space discretization, obtaining pointwise divergence free results.

2 Micropolar theory

The micropolar theory [1] adds the effects of randomly oriented particles inside the fluid to the regular Navier-Stokes model. This at the continuum scale is modeled by introducing the microrotation conservation equation. Microrotation of the particles is represented as a vector quantity that is transported and dispersed inside the fluid. It also has influence over the fluid velocity, presenting a two-way coupled, nonlinear system (1).

The following equations describe the mass, linear momentum, microrotation and energy conservation present in the micropolar theory, where we assume a steady state of the system. The problem in its strong form is to find $\mathbf{u}, p, \boldsymbol{\phi}$ and θ such that:

$$\left.\begin{aligned}
\nabla\cdot(\mathbf{u}\otimes\mathbf{u})-\nabla\cdot\boldsymbol{\sigma}(\mathbf{u},p)-2\kappa\nabla\times\boldsymbol{\phi}+\mathbf{g}\mathbf{r}\beta(\theta-\theta_0)&=\mathbf{f} && \text{in } \Omega\\
j\nabla\cdot(\mathbf{u}\otimes\boldsymbol{\phi})-\gamma\Delta\boldsymbol{\phi}-\lambda\nabla(\nabla\cdot\boldsymbol{\phi})-2\kappa(\nabla\times\mathbf{u}-2\boldsymbol{\phi})&=\mathbf{g} && \text{in } \Omega\\
\nabla\cdot(\mathbf{u}\theta)-\alpha\Delta\theta&=0 && \text{in } \Omega\\
\nabla\cdot\mathbf{u}&=0 && \text{in } \Omega\\
\mathbf{u}&=\mathbf{h} && \text{on } \Gamma\\
\boldsymbol{\phi}&=\mathbf{l} && \text{on } \Gamma\\
\boldsymbol{\sigma}(\mathbf{u},p)\cdot\mathbf{n}&=\mathbf{i} && \text{on } \Gamma\\
\theta&=m && \text{on } \Gamma
\end{aligned}\right\} \tag{1}$$

where $\boldsymbol{\sigma}(\mathbf{u},p) = -p\delta + 2(\mu+\kappa)\nabla^s\mathbf{u}$ denotes the Cauchy stress tensor for incompressible flows, having δ as Kronecker's delta and $\nabla^s\mathbf{u}$ as the symmetric tensor called the rate of deformation or strain rate tensor. Here $\mathbf{u}$ is the fluid velocity , p the fluid pressure, $\boldsymbol{\phi}$ the microrotation, θ the temperature, μ the dynamic viscosity, β the thermal expansion coefficient, α the thermal diffusivity, θ_0 the bulk temperature, γ the spin gradient viscosity, λ a viscosity coefficient ,κ the vortex viscosity, j the density of microinertia, $\mathbf{gr}$ the acceleration due to gravity, $\mathbf{f}$ are the body forces, $\mathbf{h}$ the Dirichlet boundary condition for the velocity, $\mathbf{i}$ the traction on the surface, and m the Dirichlet boundary condition for temperature.

In the system of equations (1), we have advective terms that represent the transport of a property due to the fluid motion, these are present in momentum and microrotation conservation equations, the diffusive terms that represent the transport of a property due to the differences of its concentration in space are present on all the equations except for mass conservation, and the buoyancy term that is taken as the Boussinesq approximation to represent the movement of the fluid due to density changes related to temperature variations [1, 2]. The Micropolar problem written in its weak form is to find $\mathbf{U}=\{\mathbf{u},\boldsymbol{\phi},p,\theta\}\in\mathcal{V}$ such that $\forall\mathbf{W}=\{\mathbf{w},\mathbf{z},q,s\}\in\mathcal{V}$:

$$(\mathbf{W},\mathscr{L}\mathbf{U}) = B(\mathbf{W},\mathbf{U}) = B_1(\mathbf{W},\mathbf{U}) + B_2(\mathbf{W},\mathbf{U},\mathbf{U}) = L(\mathbf{W})$$

where B_1 is a bilinear form and B_2 is a trilinear form representing the advection terms, knowing that $(\mathbf{w},\nabla\times\boldsymbol{\phi})_\Omega = (\nabla\times\mathbf{w},\boldsymbol{\phi})_\Omega + ((\mathbf{w}\times\mathbf{n})\cdot\boldsymbol{\phi})_\Gamma$:

$$\begin{aligned}
B_1(\mathbf{W},\mathbf{U}) =&(\nabla\mathbf{w},2(\nu+\kappa)\nabla^s\mathbf{u})_\Omega-(\nabla\cdot\mathbf{w},p)_\Omega-(\mathbf{w},2(\nu+\kappa)\nabla^s\mathbf{u}\cdot\mathbf{n})_\Gamma+(\mathbf{w},p\mathbf{n})_\Gamma\\
&-(\mathbf{w},2\kappa\nabla\times\boldsymbol{\phi})_\Omega+(\mathbf{w},\mathbf{g}\beta(\theta-\theta_0))_\Omega\\
&+(\nabla\mathbf{z},\gamma\nabla\boldsymbol{\phi})_\Omega-(\mathbf{z},\gamma\nabla\boldsymbol{\phi}\cdot\mathbf{n})_\Gamma+(\nabla\cdot\mathbf{z},\lambda\nabla\cdot\boldsymbol{\phi})_\Omega-(\mathbf{z},\lambda(\nabla\cdot\boldsymbol{\phi})\cdot\mathbf{n})_\Gamma\\
&-(\nabla\times\mathbf{z},2\kappa\mathbf{u})_\Omega-(\mathbf{z}\times\mathbf{n},2\kappa\mathbf{u})_\Gamma+(\mathbf{z},4\kappa\boldsymbol{\phi})_\Omega\\
&+(\nabla s,\alpha\nabla\theta)_\Omega-(s,\alpha\nabla\theta\cdot\mathbf{n})_\Gamma+(q,\nabla\cdot\mathbf{u})_\Omega\\
B_2(\mathbf{W},\mathbf{U},\mathbf{U}) =&-(\nabla\mathbf{w},\mathbf{u}\otimes\mathbf{u})_\Omega-(\nabla\mathbf{z},j\mathbf{u}\otimes\boldsymbol{\phi})_\Omega-(\nabla s,\mathbf{u}\theta)_\Omega\\
&+(\mathbf{w},\mathbf{u}\otimes\mathbf{u}\cdot\mathbf{n})_\Gamma+(\mathbf{z},j\mathbf{u}\otimes\boldsymbol{\phi}\cdot\mathbf{n})_\Gamma+(s,\mathbf{u}\theta\cdot\mathbf{n})_\Gamma\\
L(\mathbf{W}) =&(\mathbf{w},\mathbf{f})_\Omega
\end{aligned}$$

2.1 Discretization of Velocity-Pressure fields

For the discretization of our variables, we will use divergence conforming spaces to overcome the LBB condition present due to the incompressibility cons. According to the discrete differential form theory, one can build conforming spaces for operators like divergence and curl. Using these spaces, the divergence free and/or curl free conditions can be guaranteed by construction [6, 9], then using the discrete

version of these spaces leads to pointwise zero divergence or curl respectively.

Using the concept of isogeometric discrete differential forms [5] we define divergence conforming spaces using B-spline basis functions as:

Dimension	Velocity Spaces	Pressure Space
$2D$	$\mathcal{V}_h = S^{p+1,p}_{\alpha+1,\alpha} + S^{p,p+1}_{\alpha,\alpha+1}$	$\mathcal{Q}_h = S^{p,p}_{\alpha,\alpha}$
$3D$	$\mathcal{V}_h = S^{p+1,p,p}_{\alpha+1,\alpha,\alpha} + S^{p,p+1,p}_{\alpha,\alpha+1,\alpha} + S^{p,p,p+1}_{\alpha,\alpha,\alpha+1}$	$\mathcal{Q}_h = S^{p,p,p}_{\alpha,\alpha,\alpha}$

where S is the B-splines function space, p denotes the polynomial order, and α denotes the inter-element continuity. This choice of spaces can be interpreted as a smooth generalization of Raviart-Thomas elements. Assuming a polynomial order $p = 1$ and a continuity $\alpha = 0$ the discretization can be seen as implementing standard Raviart-Thomas elements, Figure 1.

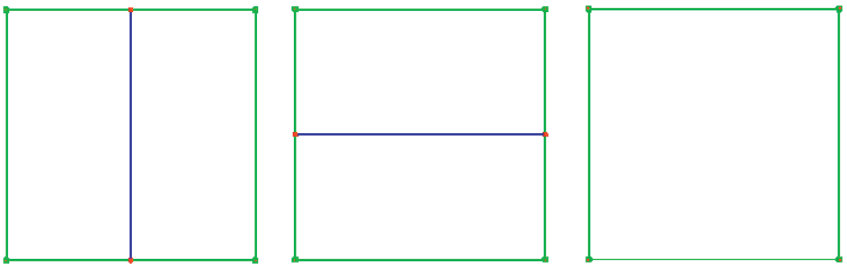

(a) X velocity element (b) Y velocity element (c) Pressure element

Figure 1: Discretization of Velocity and Pressure fields for 2D

When solving on any geometry different than the parametric, a divergence conserving transformation has to be used to relate physical with parametric space. We retain the divergence free property by using the Piola transformation when mapping the velocity, and a integral preserving mapping for the other variables, this way the following operators are introduced:

$$\begin{aligned} \mathbf{u} &= \mathcal{J}^{-1}\mathcal{F}\mathbf{U} \circ \varphi^{-1} \\ \boldsymbol{\phi} &= \mathcal{J}^{-1}\mathcal{F}\boldsymbol{\Phi} \circ \varphi^{-1} \\ p &= \mathcal{J}^{-1}P \circ \varphi^{-1} \\ \theta &= \mathcal{J}^{-1}\Theta \circ \varphi^{-1} \end{aligned}$$

where $\mathcal{F}$ is the Jacobian matrix of the parametric to physical mapping φ, Figure 2, and $\mathcal{J}$ is the determinant of $\mathcal{F}$. Variables on the parametric domain are denoted by capital letters, while physical variables are denoted by lowercase letters. To map scalar variables like p and θ the integral-preserving transformation introduces $\mathcal{J}^{-1}$ to scale the value, while for vector variables like $\mathbf{u}$ and $\boldsymbol{\phi}$, the deformation gradient $\mathcal{F}$ is also introduced in the expression to take into account the changes in the vector directions.

2.2 Boundary condition imposition

The normal boundary conditions of the velocity were imposed strongly, but doing the same for the tangential boundary conditions on the velocity, while using divergence conforming spaces can be unstable due to over restricting velocity degrees of freedom in the corners of the domain. Nitsche's method

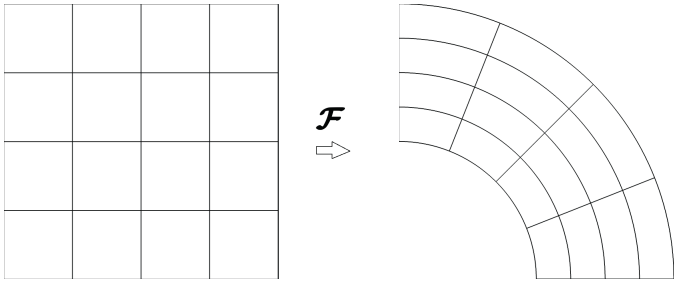

(a) Parametric domain (b) Physical domain

Figure 2: Divergence conserving mapping

for weak boundary imposition was used to avoid this problem, also alleviating the necessity for highly refined meshes to reproduce layer effects on no-slip boundaries [10].

The weak imposition of boundary conditions introduces terms to the operator $B_1(\mathbf{w}, \mathbf{u})$ and $L(\mathbf{w})$ to finally have them as in the following equations, where $\alpha_P = C_{pen}/h_f$ and C_{pen} are the penalty term parameters, h_f is the wall normal mesh size, making the bilinear operator mesh-dependent [3]. In each equation, consistency comes from the weak formulation of the problem, adjoint consistency comes from applying the adjoint operator to the consistency term, and penalisation is the term weighing velocity boundary condition $\mathbf{u} = \mathbf{h}$ [3].

$$
\begin{aligned}
B_1(\mathbf{w}, \mathbf{u}) &= (\nabla \mathbf{w}, 2(\mu + \kappa)\nabla^s \mathbf{u})_\Omega \\
&- (\mathbf{w}, 2(\mu + \kappa)\nabla^s \mathbf{u} \cdot \mathbf{n})_\Gamma && \text{Consistency} \\
&+ (\mathbf{u}, 2(\mu + \kappa)\nabla^s \mathbf{w} \cdot \mathbf{n})_\Gamma && \text{Adjoint consistency} \\
&- (\mathbf{w}, 2(\mu + \kappa)\alpha_P \mathbf{u})_\Gamma && \text{Penalisation} \\
L(\mathbf{w}) &= (\mathbf{w}, f)_\Omega \\
&- (\mathbf{h}, 2(\mu + \kappa)\nabla^s \mathbf{w} \cdot \mathbf{n})_\Gamma && \text{Adjoint consistency} \\
&- (\mathbf{w}, 2(\mu + \kappa)\alpha_P \mathbf{h})_\Gamma && \text{Penalisation}
\end{aligned}
$$

2.3 Implementation

The implementation of the concept of discrete spaces was built on top of the framework for high performance isogeometric analysis PetIGA, that provides high order, high continuity discretizations. Modifications to some structures were required so the framework could handle different discretization spaces for each variable. The implementation of Piola's transformation and integral-preserving transformation was also requeried to get divergence free discretization in the physical space. We ran all the test cases on a workstation (2 Hex-core Xeon X5650, 48 Gb memory).

3 Test problems

3.1 Heat driven square cavity

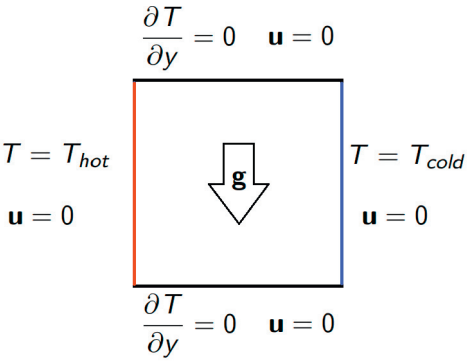

Figure 3: Heat driven cavity domain

The heat driven square cavity was used as a test case for our 2D formulation. This test presents a high temperature T_H on the right side wall, and a low temperature T_C on the left side wall. The top and bottom walls are considered to be adiabatic. No-slip and no-penetration boundary conditions are considered on every wall for the velocity [4, 7], showing how the flow is driven only by the density changes due to the heat transfer from the right to the left wall. When the velocity flow is low, isothermal lines appear as parallel to the walls, but when the velocity increases isothermal lines begin to skew towards the direction of the velocity due to the advective effects included in energy equation.

Variation of different parameters on equations (1) were computed to analize the behavior of the results. Common fluid parameters like α, μ, γ, λ and j were kept constant, the variation of the material parameter $K = \kappa/\mu$ to values of 0, 0.5 and 2, and $Ra = \mathbf{g}\mathbf{r}\beta(T_H - T_C)/\nu\alpha$ to values of $1e^4$, $5e^4$, $1e^5$, $5e^5$ were computed and compared with results from [4]. Table 1 presents streamlines results, Table 2 isothermal lines and Table 3 vorticity contours. For this test case we used a mesh of 50^2 elements with the spaces $\mathcal{V}_h = S^{2,1}_{1,0} + S^{1,2}_{0,1}$ and $\mathcal{Q}_h = S^{1,1}_{0,0}$.

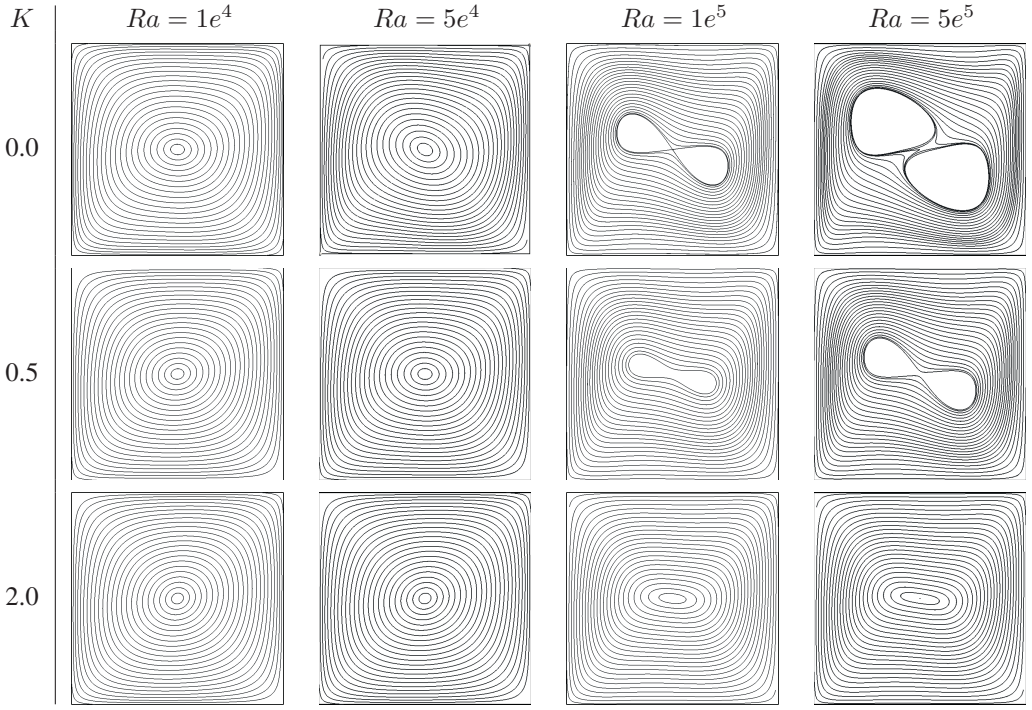

Table 1: Streamlines for different parameters K and different Rayleigh numbers ($Pr = 0.71$)

Results presented for the heat driven square cavity correspond to the ones registered by Zadravecet et al. [4], showing same behavior for Rayleigh numbers up to $1e^5$. Higher Rayleigh numbers could not be acheived with the same mesh due to the lack of implementation of an advection stabilization method. All of the results obtained a maximum divergence value of order $1e^{-9}$ according to the formulation used and the relative tolerance used in the nonlinear solver.

3.2 Heat driven arc cavity

The heat driven arc cavity was used as a test case for our divergence conserving mapping formulation. This test case presents a high temperature T_H on the bottom curved wall, and a low temperature T_C on the upper curved wall. The straight walls are considered to be adiabatic. No-slip and no-penetration boundary conditions are considered on every wall for the velocity as used in the heat driven square cavity.

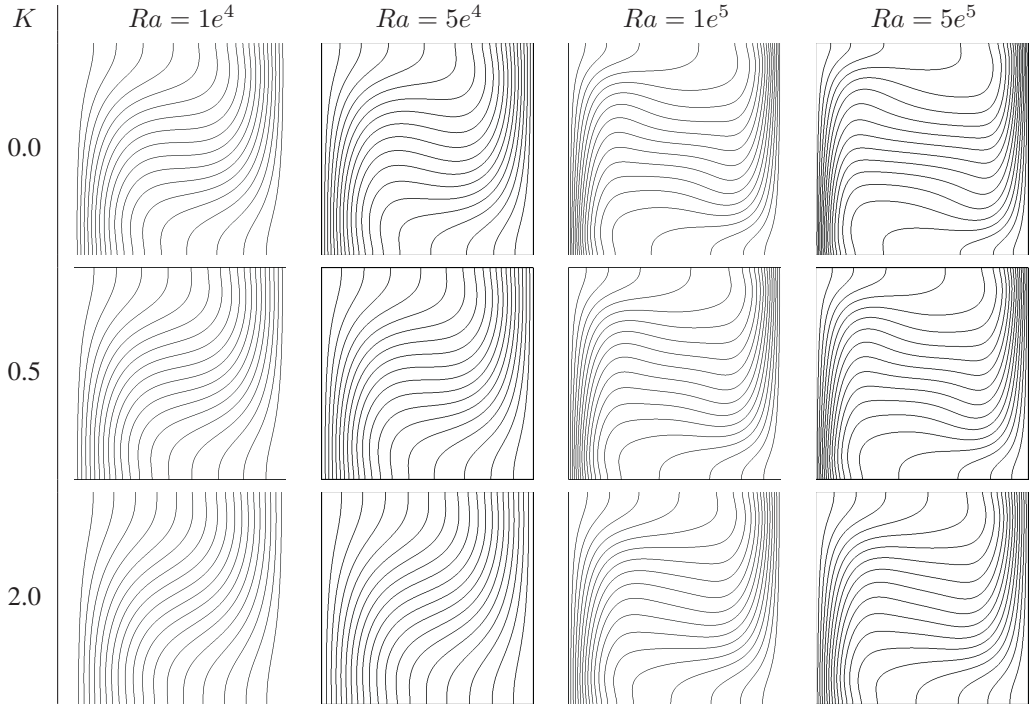

Table 2: Isothermal lines for different parameters K and different Rayleigh numbers ($Pr = 0.71$)

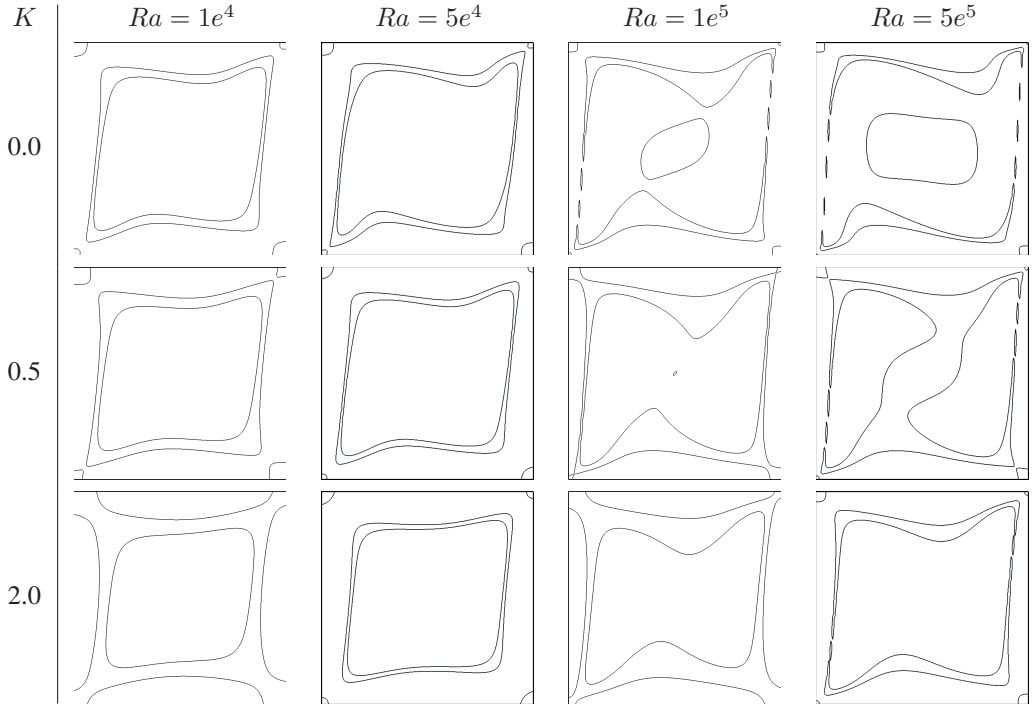

Table 3: Vorticity contours for different parameters K and different Rayleigh numbers ($Pr = 0.71$)

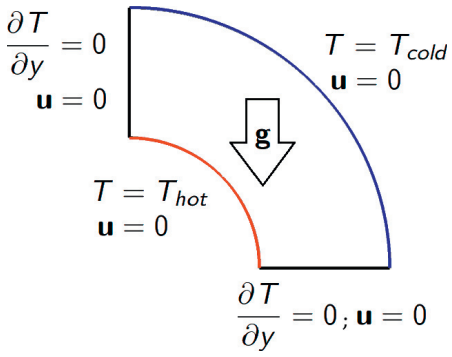

Figure 4: Heat driven cavity domain

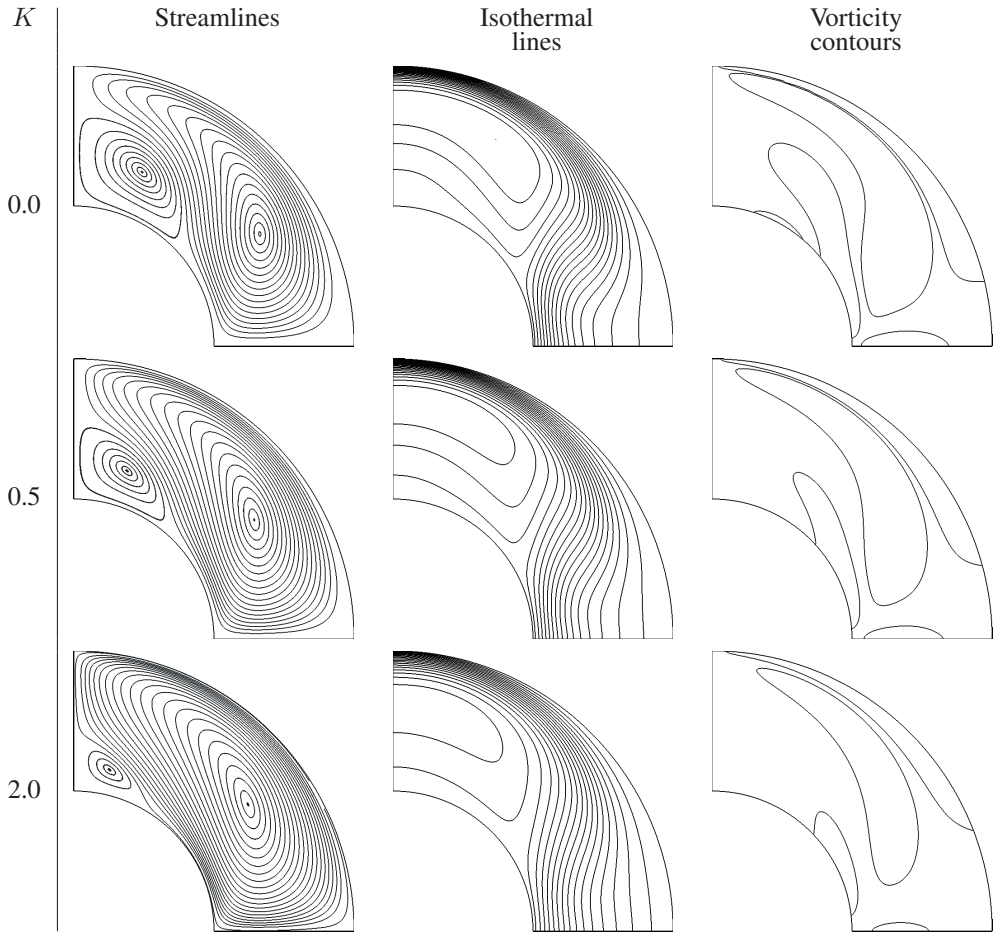

Table 4: Results for different parameters K ($Pr = 0.71$, $Ra = 5e^3$)

Only a variation of parameter $K = \kappa/\mu$ to values of 0, 0.5 and 2 were computed with a Rayleigh number equal to $5e^3$. Parameters like α, μ, γ, λ and j were kept constant. Table 4 presents streamlines,

isothermal lines and vorticity contours results, for a mesh of 50^2 elements with the spaces $\mathcal{V}_h = S^{3,2}_{2,1} + S^{2,3}_{1,2}$ and $\mathcal{Q}_h = S^{2,2}_{1,1}$.

Results for the heat driver arc cavity were not compared with any reported results. Streamlines show how fluid flows from the hot to the cold wall creating a big vortex around the cold wall and a small one around the upper part of the hot wall, this generates a higher temperature area close to the straight left wall created by the advective effects of hot fluid coming from both vortex, flowing into that specific area. Isothermal lines appear more skewed towards the cold wall due to the advection presented by the big vortex.

4 Conclusions

From the linear momentum equation we can see that in the absence of any other external force, as in the heat driven cavity problems, buoyancy is the only factor that drives the movement of the fluid. This is observed by noting that the temperature gradient between hot and cold walls is the only driving force for the fluid in both test cases.

Among the results from varying the physical parameters of the equations we found that with higher Rayleigh number, as expected, velocity increases which leads to higher effects from advective terms in the model, as seen in isothermal lines. Lack of stabilization for advection kept us from going to higher Rayleigh numbers with the same mesh. As the parameter of K is increased, velocity magnitude decreases rendering straighter isothermal lines due to smaller advection effects.

Divergence-free solutions were achieved point-wise due to the selection of our basis functions to create a divergence conformal space. This guarantees the mass conservation along the domain and an accurate solution of the flow, allowing the analysis to focus on the effect of introducing the microrotation conservation equation and how its coupling with the Navier-Stokes equations affects the results. Weak imposition of boundary conditions presents accurate results when focusing on flow near boundaries, while avoiding instabilites due to over restricting velocity degrees of freedom.

5 Future Work

Future work is to include advection stabilization with the VMS method [10], allowing us to go to higher Rayleigh and Reynolds numbers depending on boundary conditions. Going to 3D and the use of different geometries will be part of coming works, looking also for benchmarks to validate thoroughly our implementation. We will also look into including the effect over the fluid properties of adding nanoparticles, and also the addition of a transport equation for the nanoparticles in the transient case.

5.1 Acknowledgments

This work was supported by the King Abdullah University of Science and Technology KAUST, and the Numerical Porous Media Center NumPor.

References

[1] Eringen, A., *Simple Microfluids*. Journal of Mathematics and Mechanics 1964

[2] Eringen, A., *Theory of Micropolar fluids*. Journal of Mathematics and Mechanics 1966

[3] Y. Bazilevs, C. Michler, V.M. Calo and J.R. Hughes, *Weak Dirichlet Boundary Conditions for Wall-Bounded Turbulent Flows*. Computer Methods in Applied Mechanics and Engineering. 196, 2007, pp. 4853-4862.

[4] Zadravec, M., Hribersek, M., Skerget, L., *Natural convection flow of micropolar fluid in a rectangular cavity heated from below with cold sidewalls*. Engineering Analysis with Boundary Elements. 54, 2011, pp. 508518 2009

[5] A. Buffa, G. Sangalli, and R. Vasquez, *Isogeometric analysis in electromagnetics: B-splines approximation*. Computer Methods in Applied Mechanics and Engineering. 199, 2010, pp. 1143-1152.

[6] A. Buffa, J. Rivas, G. Sangalli, and R. Vasquez, *Isogeometric discrete differential forms in three dimensions*. NSIAM Journal on Numerical Analysis. 49, 2011, p. 818.844.

[7] Saleem, M., Asghar, S., Hossain, M.A., *Natural convection flow of micropolar fluid in a rectangular cavity heated from below with cold sidewalls*. . Mathematical and Computer Modelling. 54, 2011, pp. 508518 2011

[8] Hiemstra, R.R., Huijsmans, R.H.M., Gerritsma M.I., *High order gradient, curl and divergence conforming spaces, with an application to compatible NURBS-based IsoGeometric Analysis*. 2012

[9] John A. Evans and Thomas J.R. Hughes, *Isogeometric Divergence-conforming B-splines for the Darcy-Stokes-Brinkman Equations*. ICES REPORT 12-03, The Institute for Computational Engineering and Sciences, The University of Texas at Austin, January 2012

[10] John A. Evans and Thomas J.R. Hughes, *Isogeometric Divergence-conforming B-splines for the Steady Navier-Stokes Equations*. ICES REPORT 12-15, The Institute for Computational Engineering and Sciences, The University of Texas at Austin, April 2012